

Fig. 3. Output power versus frequency.

the design frequency of the choke, the output power of that diode was improved by 20 percent over the corresponding case without the choke in place. The difference in the curves at the band edges is due to a nonoptimum electrical length between cavity and choke.

The behavior of this circuit is well understood and the circuit is now being used as an analytical tool for measuring the actual Gunn diode impedance. By simply scaling the dimensions, however, it seems well suited for various system applications as well.

REFERENCES

- [1] F. M. Magalhaes and K. Kurokawa, "A single-tuned oscillator for IMPATT characterizations," *Proc. IEEE (Lett.)*, vol. 58, pp. 831-832, May 1970.
- [2] N. D. Kenyon, "A circuit design for MM-wave IMPATT oscillators," in *Int. Microwave Symp. Dig.*, pp. 300-303, 1970.
- [3] K. Kurokawa and F. M. Magalhaes, "An X-band 10-watt multiple-IMPATT oscillator," *Proc. IEEE (Lett.)*, vol. 59, pp. 102-103, Jan. 1971.
- [4] P. W. Dorman, "Gunn diode impedance measurements using a single-tuned oscillator," *Int. Microwave Symp. Dig.*, pp. 150-151, 1971.

The Accuracy of AM and FM Noise Measurements Employing a Carrier Suppression Filter and Phase Detector

JOSEPH L. FIKART, JAN NIGRIN, AND PAUL A. GOUD

Abstract—The accuracy of a commonly used noise-measuring system at microwave frequencies is calculated under actual measuring conditions. Serious deviations are shown to occur, which impose a lower and upper frequency limit on "double-channel" AM and FM noise measurements, respectively.

In laboratory systems for measurement of the AM and FM noise of microwave oscillators, the basic circuit shown in Fig. 1 is often used [1]–[4]. If the switch SW-1 is positioned such that only channel I is in operation, the circuit works as an ordinary AM detector (with the detector diodes D1 and D2 connected in phase). When both channels are used and the detector diodes are switched in opposition, the hybrid tee-diode combination operates as a phase detector and, in conjunction with the carrier suppression filter in channel II, forms a frequency discriminator for FM measurements. This "double-channel" mode of operation can also be used (at least theoretically) for AM measurements, as suggested in the literature [2], [4].

The operation of this circuit and its calibration have so far been described in terms of assumed "ideal" conditions; namely, the hybrid tee is perfect, the cavity is tuned precisely to the carrier frequency of the RF signal, and the cavity input impedance is perfectly matched at that frequency, thus producing no reflection of the carrier. The purpose of this short paper is to show how measurement accuracy is influenced in the actual case, where neither of the above criteria is satisfied.

Manuscript received December 20, 1971; revised April 17, 1972. This work was supported by the National Research Council of Canada under Grant A3725. The authors are with the Department of Electrical Engineering, University of Alberta, Edmonton, Alta., Canada.

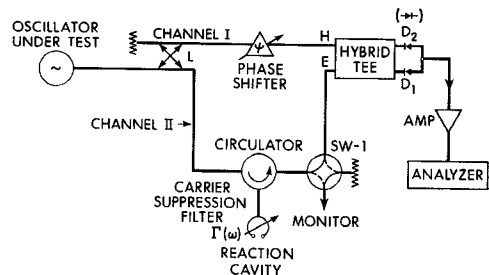


Fig. 1. Basic AM and FM noise-measuring system.

The input signal can be mathematically expressed as follows:

$$v(t) = \text{Re} \{ V_c [1 + m(t)] \exp [\omega_c t + \phi(t)] \} \quad (1)$$

where $m(t)$ and $\phi(t)$ stand for the amplitude and phase noise modulation, respectively. With $m(t) \ll 1$, $\phi(t) \ll \pi/2$, and assuming $m(t), \phi(t)$ to be truncated sample functions of wide-sense stationary processes [5], the Fourier spectrum of $v(t)$ becomes [6]

$$v(\omega) = \frac{1}{2} [V_c \delta(\omega - \omega_c) + V_c^* \delta(\omega_c + \omega)] + \frac{V_c}{2} [m(\omega - \omega_c) + j\phi(\omega - \omega_c)] + \frac{V_c^*}{2} [m^*(\omega + \omega_c) - j\phi^*(\omega + \omega_c)] \quad (2)$$

where δ is the Kronecker delta and $m(\omega) = \phi(\omega) = 0$ for $\omega \geq \omega_c$. The asterisk denotes a complex conjugate.

According to Fig. 1, the oscillator signal $v(t)$ gets to the detector diodes via two channels. The RF voltage spectrum at the respective diodes is

$$v_{D1}(\omega) = v(\omega) [L e^{j\psi} + \Gamma(\omega)] \quad (3)$$

$$v_{D2}(\omega) = v(\omega) [L e^{j(\psi + \gamma)} - (1 - A) \Gamma(\omega)] \quad (4)$$

where L is the coupling into channel I (see Fig. 1), γ is the phase inaccuracy of the hybrid tee (typically 2°), and A is the power-division imbalance of the hybrid tee (typically 0.01). The reflection coefficient $\Gamma(\omega)$ of the cavity is given by [4]

$$\Gamma(\omega) = \left(\frac{\beta - 1}{2} - jQ_0 \frac{\omega - \omega_0}{\omega_0} \right) \left(1 + jQ_0 \frac{\omega - \omega_0}{\omega_0} \right)^{-1} \quad (5)$$

where β is the cavity coupling parameter and ω_0 is its natural resonant frequency.

It can be shown by inspecting (2) that the equivalent AM noise modulation of an RF signal can be obtained from its sidebands and carrier by

$$m(\omega_m) = v(\omega_c + \omega_m)/V_c + v^*(\omega_c - \omega_m)/V_c^*. \quad (6)$$

Assuming linear detection, the Fourier component at ω_m of the balanced detector output voltage then is

$$V(\omega_m) = k \{ |c_1| m_{D1}(\omega_m) - |c_2| m_{D2}(\omega_m) \} \quad (7)$$

where c_1 and c_2 are the carrier components at diodes 1 and 2, respectively, obtained from (3) and (4) for $\omega = \omega_c$. The quantities $m_{D1}(\omega_m)$ and $m_{D2}(\omega_m)$ are obtained by applying (6) on the signal represented by (3), (4).

In the ideal case, the power spectral density $V_s(\omega_m)$ of (7) is given by

$$1) \psi = 90^\circ$$

$$V_{s1}(\omega_m) = \Delta\Omega_s(\omega_m) (\omega_m^2 + \omega_0^2/Q_0^2)^{-1} \quad (8)$$

$$2) \psi = 0^\circ$$

$$V_{s2}(\omega_m) = m_s(\omega_m) (\omega_m Q_0 / \omega_0)^2 (1 + \omega_m^2 Q_0^2 / \omega_0^2)^{-1} \quad (9)$$

where $\Delta\Omega_s(\omega_m) = \phi_s(\omega_m) \omega_m^2$ and $m_s(\omega_m)$, $\phi_s(\omega_m)$ are the power spectral densities of the AM and FM modulations. These relations are plotted in Fig. 2.

In practical measurement setups, conditions differ significantly from the ideal ones. In good systems, the hybrid tee asymmetry is within the limits indicated above, the cavity reflection at ω_c may be

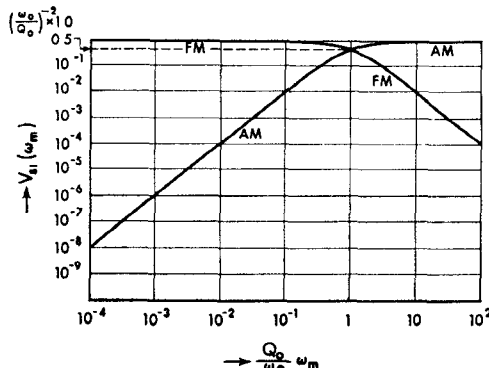


Fig. 2. Ideal case frequency dependence of $V_{s1}(\omega_m)$ normalized to $m_s(\omega_m)$ and $\Delta\Omega_s(\omega_m)$ for AM and FM, respectively.

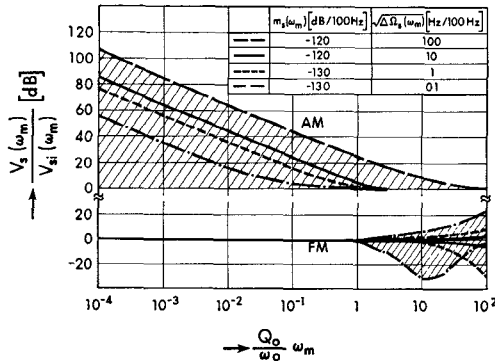


Fig. 3. Nonideal case frequency dependence of $V_s(\omega_m)$, normalized with respect to that of the ideal case, $V_{s1}(\omega_m)$, with the system parameters varying as follows: $A = 0.0$ to 0.01 , $\gamma = 0^\circ$ to 2° , $\Delta = -0.0$ to 0.01 , $\Gamma(\omega_c) = -\infty$ to -50 dB, $\Delta\psi = 0^\circ$ to 5° , $L = 0.316$ (-10 dB).

in the range $-\infty$ to approximately -50 dB, and the relative detuning of the cavity, $\Delta = Q_0(\omega_c/\omega_0 - 1)$, may vary in the range from zero to 0.01 if extreme care is taken and frequent corrections are made when tracking the measured oscillator. The error in the adjustment of ψ (maximum of "video" output for small sinusoidal deviations of the test signal is an indication) can be about $\pm 5^\circ$.

For various combinations of the above measurement conditions $V_s(\omega_m)$ has been calculated and compared with the ideal curves. The overall range of inaccuracy is plotted in Fig. 3, assuming conditions vary in the ranges indicated. The computations were carried out for four representative pairs of $m_s(\omega_m)$ and $\Delta\Omega_s(\omega_m)$, as indicated in Fig. 3. The value of L was chosen 0.316 (-10 dB), a typically used coupling. Generally, the inaccuracy increases with decreasing L . However, for FM measurements this effect is small in the range $L = 0.0$ to 0.1 (0 to -20 dB), and the overall range of inaccuracy of AM measurements is such that the effect of L is insignificant.

For the case of FM measurements, only the inaccuracy of ψ and the fact that $\gamma \neq 0$ affect to some extent the measurement accuracy at relatively high modulation frequencies. According to Fig. 3, the FM measurements can be made within a given accuracy up to a certain modulation frequency which decreases as the FM noise decreases and AM noise increases. For most oscillators to be measured, the relative modulation frequency $Q_0 f_m/f_0 = 1$ (cavity bandwidth) will be a safe limit. For a typical 6-GHz cavity with $Q_0 = 20\,000$, this corresponds to $f_m = 300$ kHz.

As can be seen from (9), even for the ideal case the AM measurement at frequencies within the cavity 3-dB points is impractical due to the large suppression introduced by the term $\omega_m Q_0/\omega_0$. A slight deviation of one of the circuit parameters from ideal conditions has a profound effect on the AM measurement accuracy, especially at modulation frequencies within the cavity 3-dB points. According to Fig. 3, the AM measurement can be made accurately from a certain modulation frequency which increases as the AM noise measured decreases and the FM noise increases. This lower limit may be as

high as $Q_0 f_m/f_0 = 10\%$. Hence it is concluded that the "double-channel" mode is unsuitable for near-carrier AM noise measurements.

REFERENCES

- [1] A. L. Whitwell and N. Williams, "A new microwave technique for determining noise spectra at frequencies close to the carrier," *Microwave J.*, vol. 2, pp. 27-32, Nov. 1959.
- [2] C. H. Grauling, Jr., and D. J. Healey, III, "Instrumentation for measurement of the short-term frequency stability of microwave sources," *Proc. IEEE*, vol. 54, pp. 249-257, Feb. 1966.
- [3] J. R. Ashley, C. B. Searles, and F. M. Palka, "The measurement of oscillator noise at microwave frequencies," *IEEE Trans. Microwave Theory Tech.*, vol. MTT-16, pp. 753-760, Sept. 1968.
- [4] J. G. Ondria, "A microwave system for measurements of AM and FM noise spectra," *IEEE Trans. Microwave Theory Tech.*, vol. MTT-16, pp. 767-788, Sept. 1968.
- [5] J. B. Thomas, *An Introduction to Statistical Communication Theory*. New York: Wiley, 1969, ch. 3.
- [6] A. B. Carlson, *Communication Systems: An Introduction to Signals and Noise in Electrical Communication*. New York: McGraw-Hill, 1968, pp. 170, 245.

A Note on Designing Digital Diode-Loaded-Line Phase Shifters

T. YAHARA

Abstract—A note is described to design digital diode-loaded-line phase shifters. A 75° separation between the loading susceptances has been shown to give the same or better performance in VSWR, loss, and phase-shift setting than a 90° separation.

The theory of operation of the diode-loaded-line phase shifter has been widely studied in the past [1]. It is well known that the ideal lossless diode-loaded-line phase-shift section and its electrical equivalent can be shown as in Fig. 1.

In Fig. 1, Opp *et al.* [2] pointed out that a $\theta = 75^\circ$ separation between the loading susceptances B rather than a 90° separation would yield the better performance in VSWR, loss, and phase-shift setting. Garver [3], however, reported that the widest bandwidth occurs around the 90° separation. If the 75° separation gives the same or better performance than the 90° one, the 75° separation has a great advantage in minimizing physical size and loss.

This short paper describes the performance of a 45° bit phase shifter comparing the two cases of the 75° and 90° separation theoretically and experimentally in the frequency range from 8.0 to 11.0 GHz. Numerical calculation was made based upon measured impedance data on leadless-inverted-device (LID) ceramic-encapsulated p-i-n diodes in the same frequency range. Experimental phase-shift networks were fabricated by thin-film techniques incorporating the same type of diodes used in the calculation.

The loading susceptances in Fig. 1 were controlled using the p-i-n diode to electrically shorten or lengthen the transmission line. The general expression for the electrical length θ' and the characteristic admittance Y_0' are given in (1) and (2), assuming lossless elements. Using these equations, the desired performance is therefore set by specifying B , Y_0 , and θ :

$$\theta' = \cos^{-1} [\cos \theta - (B/Y_0) \sin \theta] \quad (1)$$

$$Y_0' = Y_0 [1 - (B/Y_0)^2 + 2(B/Y_0) \cot \theta]^{1/2}. \quad (2)$$

The loading susceptance B as shown in Fig. 1(b) is given in (3):

$$jB = (Z_B + jZ_D \tan \theta_B)/Z_B (Z_D + jZ_B \tan \theta_B) \quad (3)$$

where θ_B is the electrical length of the stub of characteristic impedance Z_B , and Z_D is the diode impedance.

In computing the frequency dependence of the performance of the phase-shift section, electrical lengths θ and θ_B are easily calculated as a function of frequency. However, it is usually very difficult to calculate the loading susceptance B in agreement with the experimental values without using the measured diode impedance Z_D in the frequency range of interest. The impedance Z_D was therefore mea-